Available online at www.sciencedirect.com
SCIENCE DIRECT®

Journal of the European Ceramic Society 23 (2003) 2667–2670

www.elsevier.com/locate/jeurceramsoc

Study of second-phases in $Ba(Mg_{1/3}Ta_{2/3})O_3$ materials by microwave near-field microscopy

Hsiu-Fung Cheng[a,*], Yi-Chun Chen[a], Gang Wang[b], Xiao-Dong Xiang[b], Guan-Yu Chen[c], Kuo-Shung Liu[c], I-Nan Lin[c]

[a]*Department of Physics, National Taiwan Normal University, Taipei 116, Taiwan, ROC*
[b]*Intematix, Moraga, CA 94556, USA*
[c]*Department of Materials Science & Engineering; Materials Science Center, National Tsing-Hua University, Hsinchu 300, Taiwan, ROC*

Abstract

A three-dimensional (3D) finite element simulation was performed to model the behavior of the measuring resonator in an evanescent microwave probe (EMP). A calibration curve was derived using the frequency shift data as standards. The EMP measuring techniques was applied to measure the dielectric properties of $Ba(Mg_{1/3}Ta_{2/3})O_3$, BMT, materials. The average dielectric constants for these BMT materials ($\varepsilon_r = 26$–30) are consistent with the dielectric properties measured by conventional cavity method. The EMP mapping indicates clearly the presence of higher or lower dielectric constant inclusions in the one-step processed BMT materials, which contain a large proportion of secondary phases. The measurements demonstrate that the EMP method is capable of mapping the distribution of dielectric constant at very high spatial resolution.

Keywords: BMT; Dielectric properties; Microwave ceramics dielectric; Resonators; Near field spectroscopy; $Ba(Mg,Ta)O_3$

1. Introduction

The rapid growth in demand for excellent microwave dielectrics requires the development of a high-resolution microscope that can probe dielectric properties at microwave frequencies. The classical limit to the spatial resolution of any instrument based on the propagation of electromagnetic fields is $\lambda/2$, which causes the main difficulty in developing a microwave microscope. However, evanescent waves, in which the propagation of electromagnetic waves of wavelength λ decay exponentially, have spatial frequency components higher than $1/\lambda$, and have been used in near-field microscopy to achieve a spatial resolution of $\lambda/20$–$\lambda/60$[1] at different wavelengths. In this paper, an evanescent microwave probe (EMP) based on a microwave resonator[2–4] is employed to image surface impedance profiles in the microwave frequency region, and spatial resolution is further improved to ~50 nm by using a tip-probe and an efficient shielding structure.

It is difficult to obtain an analytical solution of EMP because of the complexity of the electric field distribution in the tip-sample region. To overcome this problem, a theoretical model is proposed, and a 3D finite element simulation performed to improve the accuracy of the model. Perovskite $Ba(Mg_{1/3}Ta_{2/3})O_3$ (BMT) materials, which possess highest quality (Q) factor among microwave dielectric materials, were tested by EMP in this study to verify the validity of EMP measurements.

2. Experimental methods

The structure of the evanescent microwave probe (EMP) is schematically shown in Fig. 1a; the measuring resonator consists of a sharpened metal tip, mounted on the center conductor of a high-Q (quality factor) $\lambda/4$ coaxial resonator, protruding about 500 μm beyond an aperture formed on the end wall of the resonator. A sapphire disk with a center hole of size close to the diameter of the tip wire ~50 to 100 μm and a metal layer (~1 μm) coating on the outside surface was used to shield the far-field propagating components. This design

* Corresponding author. Tel.: +886-2-29331075; fax: +886-2-29326408.

0955-2219/03/$ - see front matter © 2003 Elsevier Ltd. All rights reserved.
doi:10.1016/S0955-2219(03)00180-8

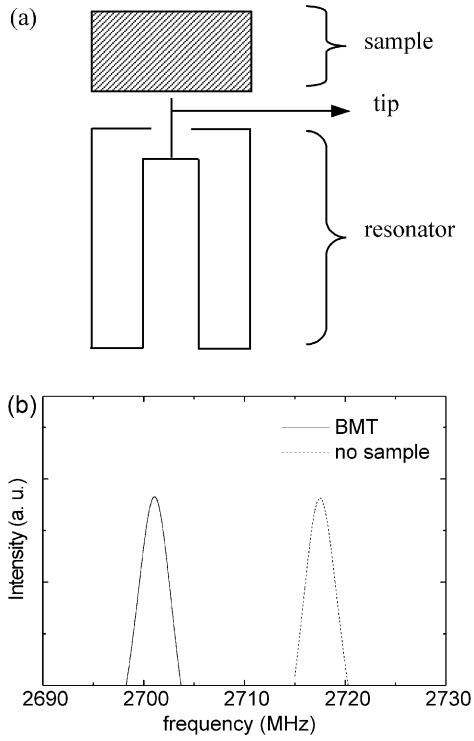

Fig. 1. (a) Sketch of a measuring resonator and (b) the typical frequency response of the measuring resonators in EMP, with or without BMT samples placed in the vicinity of measuring resonators.

minimizes the far-field background signal and allows submicron spatial resolution even in the quantitative analysis of complex dielectric constant. A change in the local environment of the probe leads to a change in resonator frequency f_0 of the resonator, and the signal is detected by measuring the power response near the resonant frequency. Fig. 1b represents the typical frequency response of an EMP measurement, illustrating the shifting of resonant frequency (f_o) for BMT ceramics with respect to the intrinsic resonant frequency of the resonator.

$Ba(Mg_{1/3}Ta_{2/3})O_3$ (BMT) materials were chosen as standard to test the validity of EMP measurements. Theses materials were prepared by conventional mixed-oxide process, which includes mixing, calcining, pulverizing, pelletizing and sintering steps. To improve the phase purity for the BMT materials, a two-step process was adopted: (1) the $MgTa_2O_5$ powders were first prepared by mixed-oxide process by calcining MgO and Ta_2O_5 mixture of 1:1 molar ratio; (2) the $MgTa_2O_5$ powders were then mixed with $BaCO_3$ in 1:3 molar ratio for nominal composition BMT and then calcined at 1200 °C. Thus obtained pure perovskite BMT powders were then palletized and then sintered at 1550 °C for 4 h. For comparison, BMT materials containing residual $Ba_5Ta_4O_{15}$ phase were also prepared, by directly calcining the $BaCO_3$, MgO and Ta_2O_5 powder mixture of 3:1:2 molar ratio, followed by pulverization, pelletization and then sintering at the same temperature.

3. Results and discussion

The measurement by EMP is based on the interaction between tip and the sample, which causes the field redistribution. To facilitate the calculation of dielectric properties from the experimental results, a theoretical model was developed. In the general case, the capacitance of the cavity is far larger than that caused by the interaction between tip and sample, so perturbation theory could be used to analyze the resonant system. Since dielectric samples are placed on the near-field region of the tip, the electromagnetic interaction can be treated as quasistatic, and the electric field inside the dielectric sample can be solved by image charge theory. Consequently, given measured f_r and Q, the dielectric properties of the materials can be calculated by using the following formula[5]:

$$\frac{\Delta f}{f_0} = -\frac{\int_v(\Delta\varepsilon E_1 \cdot E_0 + \Delta\mu H_1 \cdot H_0)\mathrm{d}v}{\int_v(\varepsilon_0 E_0^2 + \mu_0 H_0^2)\mathrm{d}v} = A\left[\frac{\ln(1-b)}{b} + 1\right] \quad (1)$$

$$\Delta\left(\frac{1}{Q}\right) = -\frac{\int_v(\Delta\varepsilon'' E_1 \cdot E_0 + \Delta\mu'' H_1 \cdot H_0)\mathrm{d}v}{\int_v(\varepsilon_0 E_0^2 + \mu_0 H_0^2)\mathrm{d}v} = -\left(\frac{1}{Q_0} + 2\tan\delta\right)\frac{\Delta f}{f_0} \quad (2)$$

where $\Delta f = f_r - f_0$, $\Delta\left(\frac{1}{Q}\right) = \frac{1}{Q} - \frac{1}{Q_0}$, f_0 and Q_0 are the resonant frequency and quality factor of the resonator when there is no sample near the tip, respectively; f_r and Q are those for resonator when a sample was placed in the vicinity of the tip. $\Delta\varepsilon = \varepsilon - \varepsilon_0$, where ε is the dielectric constant of the sample, ε_0 is the permittivity of free space, $b = \frac{\varepsilon-\varepsilon_0}{\varepsilon+\varepsilon_0}$. Due to the comlexity of the geometry for the measuring resonator, Eq. (1) can not be accurately derived. The parameter A, which is a constant determined by the geometry of the tip-cavity assembly, should be either calibrated using a standard sample or modeled numerically.

Our approach was to simulate the frequency shift of the measuring resonator by a 3D numerical analysis using Ansoft HFSS software package. The typical simulation results, which show the field distribution near the tip of measuring resonator are presented in Fig. 2. The inset in Fig. 2 clearly indicates that the electric field has highest intensity near the open end of the

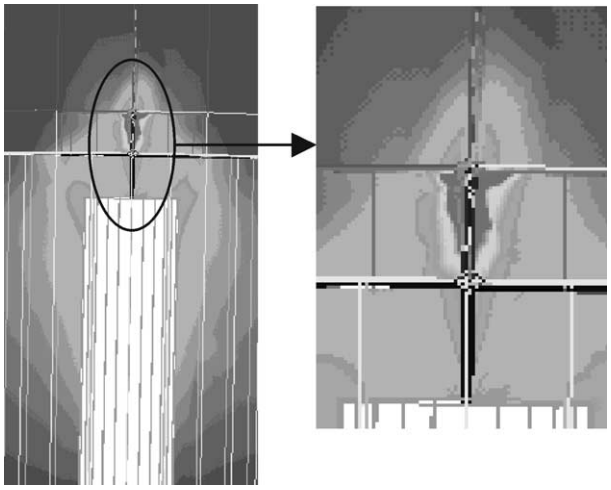

Fig. 2. Electric field distribution of EMP simulated by 3D finite element method using HFSS software.

$\lambda/4$ resonator, which is expected. The fig. also indicates that the sharp tip enhances the concentration of the field. Only a very small volume of the sample near the tip (~0.5 μm) interacts with the electric field of the measuring resonator, such that the measuring system can have very high spatial resolution and sensitivity. It should be noted that the field intensity propagating out of the resonator decays exponentially, and can only penetrates into the bulk for about 10–100 μm, depending on the dielectric constant of the sample. The higher the dielectric constant of the sample, the shallower the penetration depth. This result implies that the EMP system is sensitive enough to measure thick films, or even thin films.

The simulated frequency shifts increase with dielectric constant of the samples (Fig. 3). The A parameter in Eq. (1) was then fitted using the numerically modeled data in Fig. 3 and the variation of frequency shift with the dielectric constant of the sample is shown as the continuous curve in Fig. 3 for low dielectric region ($\varepsilon_r < 100$). Fig. 3 shows that the perturbation model fits very well with the numerically simulated results, implying that this model not only applies to samples with low ε_r values, but also is suitable for analyzing the high dielectric constant samples, such as ferroelectrics. The percentage of the frequency shift is about 0.44% when BMT sample was measured, which corresponds to a ε_r value about 26. These results are consistent with the measurements performed by conventional cavity method, indicating that our approach to calibrate the EMP measuring resonator by numerically modeling performs reasonably well.

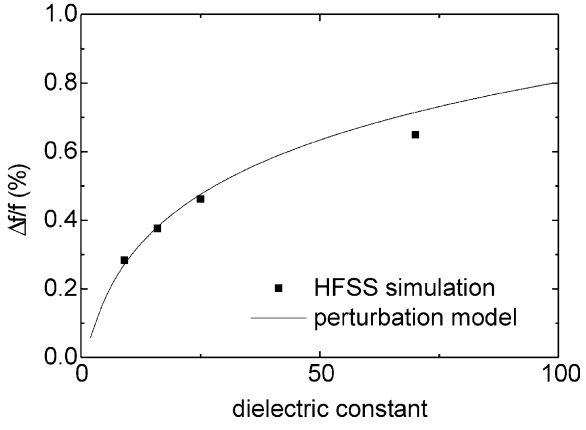

Fig. 3. The simulated frequency shift derived by HFSS simulation (solid squares) and the frequency shift versus dielectric constant curve fitted using numerically simulated data as reference standard and the formulas derived by perturbation model.

To illustrate the other feature of EMP technique, involving mapping the distribution of dielectric properties of materials in very high spatial resolution, measurements on BMT materials with or without secondary phase were performed. X-ray diffraction patterns (Fig. 4a), for BMT samples synthesized by one-step process, exhibit second phases including $Ba_5Ta_4O_{15}$, whereas Fig. 4b indicates that the BMT samples prepared by two-step process exhibit only a single perovskite phase. Microwave dielectric measurement by conventional cavity shows that pure BMT samples possess better dielectric properties ($\varepsilon_r \sim 26$, $Q \times f \sim 100{,}000$ GHz) than the samples containing second phase ($\varepsilon_r \sim 24.8$, $Q \times f \sim 48{,}000$ GHz). Fig. 5a and b show the mappings of dielectric constant derived from EMP measurements for BMT samples synthesized by one or two-step processes, respectively, and contain secondary phases or just pure perovskite. These mappings reveal that the average dielectric constant for one-step processed samples is around 27–28, which is very close to that for samples prepared by the two-step process; these data are consistent with dielectric properties measured by the conventional cavity method. However, Fig. 5a shows that the dielectric constant for one-step processed samples varies over a large range, $\varepsilon_r = 22.3$–38.3. There are regions with much higher or lower dielectric

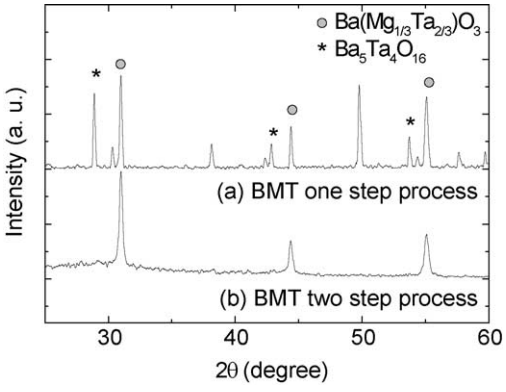

Fig. 4. (a) X-ray diffraction patterns of BMT samples synthesized by (a) one-step and (b) two-step processes.

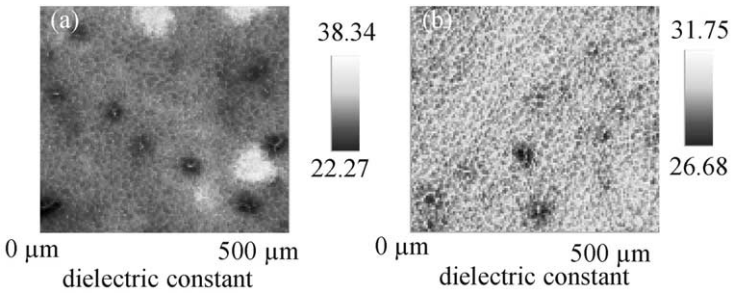

Fig. 5. Mappings of dielectric constants measured by EMP for (a) one-step processed samples and (b) two-step-processed samples.

constants than the matrix, which is in accord with the observation that there exists large proportion of second phases in the one-step-process sample. In contrast, Fig. 5b indicates that the dielectric constants of most regions in two-step processed samples are about 27–28, which is consistent with high phase purity for these BMT ceramics. These results illustrate that EMP is a useful tool for observing the spatial distribution of dielectric properties in high resolution and 3D numerical simulation can accurately model the behavior of the EMP measuring resonator.

4. Conclusions

The dielectric measurement of $Ba(Mg_{1/3}Ta_{2/3})O_3$, BMT materials were performed at microwave frequencies using a microwave near field technique, in which, the microwave evanescent field from a shielded tip on $\lambda/4$-short resonator is used to improve the spatial resolution. The dielectric constants of the samples under test were derived from the shift of resonant frequencies, which were modeled by a three-dimensional finite element simulation. The dielectric constant analyzed from the frequency shift is about 26, which is consistent with that obtained from the traditional cavity method. A sub-micrometer spatial resolution is achieved, and the dielectric properties of BMT samples with different phases in microstructure have been observed.

Acknowledgements

Financial support of National Science Council, R.O.C. through the project NSC 90-2112-M-003-028, NSC-91-2622-E-007-027 and NSC-91-2120-E-003-001 are gratefully acknowledged by the authors.

References

1. Lahrech, A., Bachelot, R., Gleyzes, P. and Boccara, A. C., Infrared near-field imaging of implanted semiconductors: evidence of a pure dielectric contrast. *Appl. Phys. Lett*., 1997, **71**, 575–577.
2. Lu, Y., Wei, T., Duewer, F., Lu, Y., Ming, N. B., Schultz, P. G. and Xiang, X. D., High spatial resolution quantitative microwave impedance microscopy by a scanning tip microwave near-field microscope. *Science*, 1997, **276**, 2004–2006.
3. Chen, G., Wei, T., Duewer, F., Lu, Y. and Xiang, X. D., High spatial resolution quantitative microwave impedance microscopy by a scanning tip microwave near-field microscope. *Appl. Phys. Lett*., 1997, **71**, 1872–1874.
4. Gao, C., Duewer, F. and Xiang, X. D., Quantitative microwave evanscent microscopy. *Appl. Phys. Lett*., 1999, **75**, 3005–3007.
5. Gao, C. and Xiang, X. D., Quantitative microwave near-field microscopy of dielectric properties. *Review of Scientific Instruments*, 1998, **69**, 3846–3851.